

1 Description of the behavior of an aquifer by using
2 continuous radon monitoring in a thermal spa

3 © 2016. This manuscript version is made available under the CC-BY-NC-ND 4.0 license [http://creativecommons.org/licenses/by-nc-](http://creativecommons.org/licenses/by-nc-nd/4.0/)
4 [nd/4.0/](http://creativecommons.org/licenses/by-nc-nd/4.0/)

5 *Carlos Sainz ^{*1}, Daniel Rábago¹, Ismael Fuente¹, Santiago Celaya¹, Luis Santiago Quindós-¹*

6

7 ¹ Faculty of Medicine, University of Cantabria, Spain.

8 *Corresponding author:

9 Carlos Sainz-Fernandez

10 Cátedra de Física Médica Departamento de Ciencias Médicas y Quirúrgicas

11 Facultad de Medicina, Universidad de Cantabria

12 Avda. Herrera Oria s/n, E-39011 Santander, Cantabria, Spain

13 Tel.: +34942201976

14 E-mail: sainzc@unican.es

15

16 Keywords: radon concentration, thermal water, aquifer, spa, occupational exposure

17

18 **Abstract**

19 Radon (^{222}Rn) levels in air and water have been analyzed continuously for almost a year in
20 Las Caldas de Besaya thermal spa, north Spain. Radon is a naturally occurring noble gas from
21 the decay of radium (^{226}Ra) both constituents of radioactive uranium 238 series. It has been
22 recognized as a lung carcinogen by the World Health Organization (WHO) and International
23 Agency for Research on Cancer (IARC). Furthermore the Royal Decree R.D 1439/2010 of
24 November, 2010 establishes the obligation to study occupational activities where workers and,
25 where appropriate, members of the public are exposed to inhalation of radon in workplaces
26 such as spas. Together with radon measures several physico-chemical parameters were
27 obtained such as pH, redox potential, electrical conductivity and air and water temperature.
28 The devices used for the study of the temporal evolution of radon concentration have been the
29 RTM 2100, the Radon Scout and gamma spectrometry was complementarily used to determine
30 the transfer factor of the silicone tubes in the experimental device. Radon concentrations
31 obtained in water and air of the spa are high, with an average of 660 Bq/l and 2900 Bq/m³
32 respectively, where water is the main source of radon in the air. Radiation dose for workers
33 and public was estimated from these levels of radon. The data showed that the thermal
34 processes can control the behavior of radon which can be also influenced by various physical
35 and chemical parameters such as pH and redox potential.

36

37

38

39

40

41 **1. Introduction**

42 Radon (^{222}Rn) is a naturally occurring radioactive gas that has a half-life $T_{1/2}$ of 3.8 days. It
43 is formed as the decay product of radium (^{226}Ra) with $T_{1/2}=1600$ years, which is a member of
44 the radioactive series of uranium (^{238}U) (1). Uranium and radium found naturally in soil and
45 rocks, provide a continuous source of radon. Because of its gaseous nature, radon is able to
46 escape from the rock depending on the density and porosity thereof, being one of the most
47 common radioactive elements in groundwater (2).

48 Under normal conditions, radon has a density of 9.73 kg/m^3 , making it the densest gas of
49 nature (7). Of all noble gases, it is the most soluble in water. Owing to the nature of noble gas,
50 its behavior is determined by physical processes. However its parent ^{226}Ra is highly reactive,
51 it forms compounds as Ra^{2+} . Radium constitutes an efficient radon source when once dissolved,
52 is absorbed by the surface of rocks and minerals of the aquifer (3), thus avoiding loss or diluting
53 the concentration of radium in water during high flow processes or aquifer recharge.

54 Some hot springs have high concentrations of radium and radon. For example, studies in
55 Spanish spas provide radon concentrations in water above 1800 Bq/l and 36 Bq/l for radium
56 (4). The release of radon through water spas in the environment may be a risk to the health of
57 workers of thermal installations as well as for patients (5, 7).

58 When radon is inhaled, its disintegration products (^{218}Po and ^{214}Po) are deposited in lungs,
59 they emit alpha particles which could interact with biological tissues causing DNA damage (6).
60 Due to its gaseous nature, which makes it possible to build up in enclosed spaces such as homes,
61 spas, caves or mines, reaching high concentrations. In 1988 radon was classified as a human
62 carcinogen by the International Agency for Research on Cancer (IARC), agency specializing
63 in cancer research within WHO, from epidemiological studies of uranium miners (7). Currently
64 radon is recognized as the second cause of lung cancer in the population after tobacco (6).

65 According to United Nations Scientific Committee on the Effects of Atomic Radiation
66 (UNSCEAR), the average dose received by the Spanish population is 3.7 mSv/year, which 2.4
67 mSv are due to natural radiation (the global value) where 1.3 mSv are relevant to radon (8).

68 This study focuses on two objectives. Both are based on continuous measurement of
69 dissolved radon (^{222}Rn) in water and radon concentration in air of thermal facility, as well as
70 of physical and chemical parameters.

71 The main objective is based on the characterization of the source of radon in the indoor air
72 in the thermal spa. To do this, dissolved radon in water as natural tracer was monitored to
73 evaluate transfer dynamics to air, to determine the aquifer dynamics and find the radon sources
74 in the thermal installation. The second objective focuses on radiological protection of the
75 workers and patients from the risks derived of radon inhalation. In addition, the concentrations
76 found in air are compared with reference levels detailed in Spanish legislation (IS-33
77 instruction): if the annual average radon concentration is lower than 600 Bq m^{-3} no specific
78 control is needed; if it is between 600 and 1000 Bq m^{-3} it must be applied a low level of control
79 (follow up of annual average concentration), and if it is higher than 1000 Bq m^{-3} , a high level
80 control must be implemented, which can be related with administrative/technical interventions
81 in order to reduce the exposure of workers (9).

82 **2. Materials and methods**

83 **2.1 Site description**

84 Las Caldas de Besaya thermal spa is located beside the river Besaya in the village Los
85 Corrales de Buelna ($43^{\circ}17'53''\text{N}$, $4^{\circ}04'23''\text{O}$) about 30 km from Santander, the capital of the
86 autonomous community of Cantabria, Spain (Figure 1). Thermal water of this spa is
87 characterized by a temperature between $34\text{-}37 \text{ }^{\circ}\text{C}$, a sodium-chloride composition,
88 bicarbonated and nitrogenous (10).

89 The rock type in this area has sedimentary origin, the most part gray limestone and dolomite
90 (11). Although the susceptibility of Cantabrian lithologies to release radon is very low (12), the
91 thermal facility is located over an inverted basin geological fault called “Frente Cabalgante del
92 Escudo de Cabuérniga”, which runs parallel to the coast. Several natural springs of thermal
93 water are present along this fault and its relationship with the presence of high radon
94 concentrations in water, as well as a more detailed description of the structural geology in the
95 Cantabria region can be found in (13)

96 The period of annual opening of the resort is usually from March to December. It has many
97 services and treatment techniques as baths, jets, circular showers, bubble baths, inhalations,
98 sprays, sauna, underwater massage and manual massage.

99 In the thermal spa there are seven hot springs. The connection between them remains
100 unknown and could be an interesting topic for future studies. To supply services, water is
101 regularly pumped (from 6:00 a.m. to 12:00 p.m.) from a well located outside of the installation,
102 and part of this water is mixed with the water of the main well where measurements were
103 performed.

104 **2.2 Sampling and experimental device**

105 Radon levels were determined inside thermal spa by measuring the gas concentration in
106 water and air. Radon concentration in water, which outcrops at thermal spa, was measured
107 every hour over five months, between March and August 2012. In the case of radon
108 concentration in air the measures were extended until February 2013.

109 To determine the concentration of radon dissolved in water $C_{Rn,water}$ it has been used two
110 methods. The first was performed continuously by the device RTM 2100 (Sarad GmbH,
111 Germany) which scheme is shown in Figure 2. The whole system consists in a closed air circuit
112 by which air is continuously circulating through the semiconductor-based detection chamber

113 of the RTM device by means of a low flow pump. The outside part of the air circuit is made of
114 a silicone, which is highly permeable to radon. In addition, the measurement system of radon
115 in water was studied in relation to diffusion tubes. The material and length of the tubes were
116 changed in order to increase the efficiency of radon diffusion transfer.

117 When around 2 m of these tubes (3 mm of inner diameter and 1 mm of thickness) are
118 submerged into the water contained in the vessel of 3 l volume, a given amount of radon
119 dissolved in the liquid is passing by diffusion to the closed air circuit. Taking to account that
120 the detection efficiency of RTM is highly sensitive to absolute humidity, and in order to avoid
121 water condensation into the detector chamber, a Peltier dryer is placed nearby the entrance of
122 air into the RTM device. Moreover, to prevent entrance of liquid water into the system in case
123 of accident, a compensation bottle is also placed in front of the dryer.

124 The second method was based on grab sampling and determination by gamma spectrometry
125 technique. Samples were collected every week, filling containers slowly in order to minimize
126 water turbulences and subsequent radon losses by desorption. For the determination of ^{222}Rn
127 concentration in water, hermetically sealed containers made from polyethylene were used for
128 sample collection, and measured with a high-purity Ge coaxial detector, with a relative
129 efficiency of 20 %. Its resolution was 1.86 keV and it is logged inside a low activity iron casing.
130 The samples were measured once the equilibrium between ^{222}Rn and its progeny was reached,
131 3 hours after the sample collection, using the 609 keV photopeak of ^{214}Bi . The sampling and
132 measurement procedures have been described in detail elsewhere (4).

133 Continuous measurement of radon concentration in air $C_{\text{Rn,air}}$ inside the spa were performed
134 with the Radon Scout device (Sarad GmbH). Water samples were taken the main well while
135 the Radon Scout device was located one meter away. Several physico-chemical parameters as
136 electrical conductivity, redox potential and pH were taken together with radon concentration

137 measurements by means of independent probes integrated in the measuring system. Water and
138 air temperatures have also been monitored. The accuracy of radon measurement system was
139 recently tested by participating on international intercomparison exercise (14)

140 **2.3 Determination of transfer factor**

141 Radon concentration provided by RTM 2100 is expressed in Bq/m³ because this device
142 measures radon concentration in the air circuit (see Figure 2). In order to find a suitable transfer
143 factor from radon in water to radon in air concentration, the above indicated gamma
144 spectrometry measurements from grab samples were made. Although the transfer factor is
145 dependent of water temperature (15), it has been found that in case of the studied aquifer this
146 parameter is practically constant, ranging less than 0.5 °C during the observed period. For this
147 reason, the influence of temperature could be neglected in this study. Determinations by gamma
148 spectrometry at the laboratory of environmental radioactivity of the University of Cantabria
149 (LARUC) are continuously validated with ISO based quality assessment, as well as by
150 participating successfully in international exercises of intercomparison (14). Therefore to
151 obtain radon concentration in water expressed in Bq/l, the gamma spectrometry results have
152 been compared with RTM 2100 ones. Additional low level radon concentration in water
153 obtained from our laboratory where used to complete the relationship for a broader range of
154 concentrations. Linear fit of the Figure 3 provides the transfer factor *tf*:

$$155 \quad C_{\text{Rn}}(\text{gamma}) = tf \cdot C_{\text{Rn}}(\text{RTM}) \Rightarrow tf = (1,96 \pm 0,10)10^{-4} \frac{\text{Bq/l}}{\text{Bq/m}^3} \quad (1)$$

156 This value of transfer factor is higher than the solubility coefficient of radon in water at
157 around 36 °C (typical water temperature in the studied facility) (15) because of the radon
158 gradient inside the wall of the tube provoked by diffusive process.

159 **2.4 Radon behavior models**

160 Two different mathematical models were used to explain the variations of radon concentration
 161 observed continuously in the main well. The models were fed with the temporal series of radon
 162 concentrations measured in water, and then the fitting parameters used in these models have
 163 provided additional information, as the rate of water exchange between the main well and other
 164 secondary wells, or the degree of radon loss in the water-air interface per unit time.

165 **2.4.1 Closed Compartment Model (CCM)**

166 This model tries to explain the radon concentration variation with the time when the thermal
 167 spa is without activity (treatments, etc...) (from 12 PM. to 6 AM). When external water is not
 168 pumped, main well doesn't received water from outside.

169 Closed Compartment Model supposes that it has a volume of water V with an initial radon
 170 concentration $C_{\text{Rn,water}}(t=0)$ named as C_0 . Inside that water volume there is a radon source with
 171 a exhalation rate E and surface S . Radon concentration decrease is given by disintegration to
 172 and passage of radon dissolved in water to air. Therefore radon concentration dynamics (16) is
 173 set as:

$$174 \quad \frac{dC_{\text{Rn,water}}}{dt} = \phi - \lambda C_{\text{Rn,water}} \quad (2)$$

175 where $\lambda = \lambda(^{222}\text{Rn}) + \lambda_v$ [h^{-1}], $\lambda(^{222}\text{Rn}) \equiv ^{222}\text{Rn}$ decay constant, $\lambda_v \equiv$ constant that reflects the
 176 radon loss in water-air interface per unit time, $\phi = ES / V \equiv$ radon emission rate [Bq/l h^{-1}].

177 The variation of radon concentration in water over time is given by the resolution of the
 178 equation 2:

$$179 \quad C_{\text{Rn,water}}(t) = C_0 e^{-\lambda t} + \frac{\phi}{\lambda} (1 - e^{-\lambda t}) \quad (3)$$

180 The asymptotic radon concentration in water C_{max} can be obtained with the next condition:

181
$$\frac{dC_{\text{Rn,water}}}{dt} = 0 \Rightarrow C_{\text{max}} = \frac{\phi}{\lambda} \quad (4)$$

182 **2.4.2 Opened Compartment Model (OCM)**

183 This model tries to explain the radon concentration variation with the time when the thermal
 184 spa is working (from 6 AM to 12 PM). In this case water with radon concentration C^* is
 185 pumped from outside, the main well receives part of this water. Model conditions are identical
 186 to CCM ones but it is necessary add an exchange term λ_l . Thus radon concentration dynamics
 187 in water (16) is given by:

188
$$\frac{dC_{\text{Rn,water}}}{dt} = \phi - \lambda C - \lambda_l (C_{\text{Rn,water}} - C^*) \quad (5)$$

189 The above equation resolution with the initial condition $C(t=0)$ named as C_1 is:

190
$$C_{\text{Rn,water}}(t) = C_1 e^{-\lambda^* t} + \frac{d}{\lambda^*} (1 - e^{-\lambda^* t}) \quad (6)$$

191 Where $d = \phi + \lambda_l C^*$ [Bq/l h⁻¹] and $\lambda^* = \lambda + \lambda_l$ [h⁻¹].

192 From adjustment parameters obtained in the CCM and OCM models shown in Table 1,
 193 exchange constants per unit time λ_l and λ_l have been calculated, and the estimation of radon
 194 concentration of outside well was used for testing the model. The result of fitting the
 195 experimental data on the radon concentration in water with the Closed and Opened
 196 Compartment Models referred to the first time series of Table 1, is shown in Figure 4.

197

198 **2.5 Dose estimation**

199 The effective dose rate expressed in mSv per period time was estimated from the following
 200 equation:

201
$$\dot{H}[\text{mSv/period}] = \text{WLM} \cdot f \quad (7)$$

202 with f conversion factor whose value to the public and workers is 4 and 5 mSv/WLM
203 respectively. The unit WLM (Working Level Month) is defined as exposure to 1 WL for a work
204 period of one month (170 h):

205
$$\text{WLM} = \frac{\text{WL} \cdot t(\text{h/period})}{170} = \frac{C_{\text{Rn,air}}(\text{Bq/m}^3) \cdot F}{3700} \quad (8)$$

206 where F is the equilibrium factor between radon and its progeny (17). According to UNSCEAR
207 for typical residential environments takes an average value of 0.4 (18).

208 **3. Results and discussion**

209 **3.1 General results**

210 As shown in Figures 5, 9 and 10, radon levels in water and air of Las Caldas de Besaya
211 thermal spa are highly variable. Radon in water average is 660 Bq/l with maximum and
212 minimum of 764 and 306 Bq/l respectively, while the radon in air average is 2900 Bq/m³ with
213 10400 and 890 Bq/m³ maximum and minimum values respectively in the months studied. One
214 of the highest levels of Spain according to the article by Soto et al. (23) which shows the results
215 achieved from measurements performed in 54 spas.

216 Dose estimation was obtained from equation 7, 8 and the average value of radon
217 concentration in air, 2900 Bq/m³ whose maximum and minimum are 10400 and 890 Bq/m³
218 respectively. Dose calculate was done annual and monthly for workers with 2000 and 170 hours
219 spent on the installation respectively. In the case of patients, dose was calculated for a week
220 with 2 hours of permanence per day. However, as these dose estimations have been made under
221 the assumption of standard working conditions, which do not fit perfect with the specific
222 conditions of this workplaces, it would be necessary to monitor radon in air in each area and

223 include personal dosimeters to workers in order to obtain more accurate and reliable values
224 (20).

225

226 **3.2 CCM and OCM models**

227 Radon concentration in water usually has a periodic behavior with minimum values reached
228 usually in the beginning of the afternoon during working days, and the highest ones around 7-
229 8 AM in the same days. The models described in section 2.4 try to explain this periodicity.

230 Radon behavior in water seems to be well explained by the proposed models CCM and
231 OCM. Experimental data are adjusted accurately by equations models. In all cases the adjusted
232 coefficient of determination R^2 -adj is not less than 0.94.

233 Several conclusions can be drawn from the CCM model results. Losses of radon in water
234 are mainly controlled by the desorption air through the water surface ($\lambda \approx \lambda_v$), making water
235 the main source of radon at spa. Emission rate ϕ takes a mean value of 260 ± 60 Bq/l h⁻¹, value
236 that could be taken as reference to characterize the main well. However it has high variability
237 and might not be constant over year, can be controlled by other factors such as the flow of
238 water coming out the spring that supplies the main well.

239 From OCM model radon concentration of outside well C^* have been obtained (see Table 2)
240 being most of results consistent with 560 ± 80 Bq/l the article of Soto and colleagues (22, 23).
241 This model has also allowed characterizing the exchange of water volume per unit time through
242 constant λ_r between the main well and the outside one, and λ_v , which indicates the radon loss
243 in water-air interface per unit time.

244 **3.3 Anomalies in water radon concentration**

245 It have been found several anomalies, which means, from the point of view of radon
246 concentration in water, a behavior which CCM and OCM models are unable to explain. Figure
247 5 shows radon concentration in water and a number of physico-chemical parameters, periodic
248 behavior is observed except in shaded area (on April 8 and 14 to 17). Concentration in both
249 periods was higher, in the second range periodicity given by the OCM model did not appear.
250 Further water temperature and conductivity were significantly decreased this period.

251 In period where anomalies were observed, thermal spa was closed, i.e., water from outside
252 well was not pumped. Therefore, OCM model does not determine radon dynamics in this case.
253 It is remarkable that radon desorption to air through the water surface depends on the
254 temperature thereof (19).

255

256 **3.4 Relationship between radon in water and radon in air**

257 To determine the relationship between radon in water and air concentrations, a correlations
258 study has been carried out. For April, radon concentration is inversely correlated, for the other
259 months there is no correlation. Figure 6 shows anticorrelation between water and air radon,
260 furthermore shaded area indicates the period where anomalies in water radon concentration
261 were found. As mentioned in previous sections, the daily maximum radon concentration in
262 water appears around 7-8 AM when activity of the spa begins, and pump bringing fresh water
263 into the main well starts working. At the same time, services such as jets, showers or inhalations
264 also begin increasing the concentration of radon in air gradually by desorption from the water.
265 The high variability of radon concentration in air corresponding to the seasonal end, could be
266 attributable to storms and flood events in the thermal spa. Moreover, that variability indicates
267 the adequacy of continuous monitoring when precise radiological protection have to be made.
268 However, it would be necessary a larger number of measuring points given the large volume

269 and spaces within the spa to know more accurately radon in air dynamics. The influence of this
270 kind of events on radon in water and radon in air concentrations should be afforded in more
271 detail in further studies.

272 **3.5 Correlations with physico-chemical parameters**

273 Correlations study was made between the radon concentration in water and physico-
274 chemical parameters, as well as radon concentration in air with air temperature. Some inverse
275 correlations were found between radon in water and pH and air temperature. On the other hand,
276 positive correlation was observed between radon in water and redox potential and, between
277 radon in air and air temperature. Correlations with conductivity and water temperature were
278 not found.

279 Theoretical models explain quite well the radon behavior in water, it is basically controlled
280 by the operation of the spa. However conductivity and water temperature decrease when the
281 spa is closed (see Figure 5). These parameters are related with the origin of water, showing the
282 main well lower values than those corresponding to the outside well. Leaks from rain or river
283 would decrease greatly conductivity and water temperature. Radon solubility decreases with
284 temperature, accordingly outside well has less radon than the main, assuming the same radium
285 content in rocks of both.

286 One of the conclusions that have been mentioned is that the radon source in air is water.
287 Nevertheless radon behavior in air has high variability and it can be controlled by many factors
288 as ventilation, number of patients using the facilities, atmospheric pressure, etc. There is direct
289 correlation between radon in air and air temperature, this may be due to the operation of the
290 spa. And a low inverse correlation between radon in water and air on April, being insignificant
291 for the other months, which does not lead to a reliable result.

292 Analyzing the correlations of the radon concentration in water with the other parameters
293 measured, it has been found that the pH and redox potential have moderately and high direct
294 correlation respectively. Those conditions are suitable for the radio solution (Ra^{2+}) is absorbed
295 by the aquifer surface, thus constituting an excellent source of radon. There is a high inverse
296 correlation with air temperature that as in the previous case may be due to operation of the spa.
297 With water temperature would expect an inverse correlation, but as variations of it are the order
298 of the thermometer uncertainty, no significant results were found.

299

300 **3.6 Dose estimation**

301 IS-33 instruction establishes 600 Bq/m^3 as reference level of radon concentration in air.
302 Levels at Las Caldas de Besaya thermal spa far exceed this level, establishing above 1000
303 Bq/m^3 , which would lead applying a high level of control. In this situation, the general
304 principles of operational radiation protection under Title IV of RPSRI (23) must be applied. In
305 practice, this implementation will take place gradually, considering the level of exposure, the
306 number of workers affected and existing protection alternatives. It should be studied the radon
307 concentration in air in all places where workers are commonly found, in order to know more
308 precisely the characteristic dose of each working activity. Dynamics knowledge of radon
309 concentration in indoor air would apply radiation protection systems based on changes in work
310 schedule.

311 According to the dose estimation to workers and public, the first could receive in a year of
312 work up to 18 mSv , over 7 times the annual global average dose associated with natural
313 radiation. They will receive the global average doses associated with radon in a month working
314 at spa. In case of patients the dose received in a week would be the equivalent of a chest

315 radiograph, ranging around 0.1 mSv per week, a contribution to the annual dose of little
316 relevance.

317

318

319 **4. Conclusions**

320 Continuous radon monitoring have been performed continuously for almost a year in the
321 indoor air and water of a thermal spa located in the North of Spain. With an integrated
322 measuring system, also other parameters like temperature, pH or conductivity were monitored
323 in water as well. The system was set up for the specific measuring conditions by means of
324 validated gamma spectrometry technique for radon in water analysis. The system can be used
325 in a wide variety of scenarios where radon in water monitoring is required, but a good
326 determination of the transfer factor of the diffusive tubes corresponding to the specific water
327 temperatures of each case should be carried out .

328 It was observed that radon concentration in water usually showed a periodic behavior,
329 related with the daily operation of the thermal facility. In order to explain it, two simple
330 theoretical models were successfully applied. The equations given by these models are
331 adjusted to the experimental data quite accurately. From CCM (closed compartment model) it
332 can be concluded that the loss of radon in water are controlled mainly by radon desorption to
333 the indoor air through the water surface. At the same time, this fact points out the free water
334 surface inside the facility as a major source of indoor air radon concentration. However, more
335 detailed measurements of radon in air should be performed in different rooms for treatment in
336 order to refine this conclusion, as the concentration of radon in air can be significantly
337 influenced by a number of other factors such as ventilation, the work of showers, jets, and other
338 techniques used in the spa.

339 On the other hand, the results obtained from the application of OCM (open compartment
340 model) provided an approximation of the radon concentration in the outer well which supplies
341 the facilities. Most values obtained were consistent with previous results present in literature.
342 This model also allowed characterizing the exchange of volume per unit of time with constant
343 water between the main well and the outer one.

344 The measurement of additional parameters like conductivity and water temperature
345 have provided some relevant information about the origin of water. For example, the water
346 from the river or rain usually can present lower conductivity and very low temperature
347 compared to thermal water, causing decreases in these two parameters when it is pumped to
348 the main well. Analyzing the correlations of the radon concentration in the water with the other
349 parameters measured, it was found that the pH and redox potential have a moderate to high
350 direct correlation respectively. However, the correlations found have to be studied more in
351 depth in order to obtain a conclusion with applicability to other projects or applications.

352 Finally, and according to Spanish regulation related with exposure to radon in workplaces,
353 a preliminary dose assessment was done for workers and public. The annual average indoor
354 radon concentration indicate that it would be necessary to apply the principles of operational
355 radiological protection established in Title IV of RPSRI (22). In practice, this implementation
356 would take place gradually, considering the level of exposure, the number of workers affected
357 and the existing alternatives protection.

358 **5. Acknowledgements**

359 Authors would like to express their gratitude to the director of the facility for allowing the
360 development of measurements inside the thermal installation. Any additional data apart from
361 the presented in the tables and figures of this manuscript may be obtained by request from Prof.
362 Carlos Sainz (email: sainzc@unican.es).

363

364

365 **6. References**

366 (1) Nazaroff W.; Nero A.; Radon and its decay products in indoor air. Ed. Wiley & Sons,
367 **1988** ISBN: 0-471-62810-7

368 (2) Roba, C. A.; Nita, D.; Cosma, C.; Codrea, V.; Olah, S. Correlations between radium and
369 radon occurrence and hydrogeochemical features for various geothermal aquifers in
370 Northwestern Romania. *Geothermics*. **2012**, *42*, 32-46; DOI
371 10.1016/j.geothermics.2011.12.001

372 (3) Surbeck, H. Dissolved gases as natural tracers in karst hydrogeology; radon and beyond.
373 *Proceedings of Multidisciplinary approach to Karstwater Protection Strategy. UNESCO*
374 *Course*. **2005**.

375 (4) Rodenas, C.; Gómez, J.; Soto, J.; Maraver, F. Natural radioactivity of spring water used
376 as spas in Spain. *Journal of radioanalytical and nuclear chemistry*. **2008**, *277* (3), 625-
377 630; DOI 10.1007/s10967-007-7158-3.

378 (5) Welch, L.; Mossman, D. An Environmental Chemistry Experiment: The Determination
379 of Radon Levels in Water. *Journal of Chemical Education*. **1994**, *71* (6), 521-523; DOI
380 10.1021/ed071p521

381 (6) WHO handbook on indoor radon: a public health perspective [Internet].

382 Geneva: World Health Organization; 2009. Available online:
383 <http://www.ncbi.nlm.nih.gov/books/NBK143216/>

- 384 (7) International Agency for Research on Cancer. *IARC monographs on the evaluation of*
385 *carcinogenic risks to humans, Man-made Mineral Fibres and Radon*. International
386 Agency for Research on Cancer: UK, **1988**; 43.
- 387 (8) UNSCEAR. *Sources and effects of ionizing radiation, UNSCEAR 2000 Report*; United
388 Nations Scientific Committee on the Effects of Atomic Radiation: New York, **2000**;
389 *Volume I: Sources*.
- 390 (9) Consejo de Seguridad Nuclear. *Instrucción IS-33, Sobre Criterios Radiológicos Para la*
391 *Protección Frente a la Exposición a la Radiación Natural*; Boletín Oficial del Estado
392 (BOE): Spain, **2012**; 22.
- 393 (10) Agencia de Evaluación de Tecnologías Sanitarias (AETS) Instituto de Salud Carlos III -
394 Ministerio de Sanidad y Consumo, Hernández, A. et al. *Técnicas y Tecnologías en*
395 *Hidrología Médica e Hidroterapia*; AETS - Instituto de Salud Carlos III: Madrid, **2006**.
- 396 (11) Robador, A.; Heredia, N.; Rodríguez, L. R.; Marquinez, J. *Mapa geológico de Cantabria,*
397 *Escala 1:100000*. Instituto Geológico y Minero de España: Madrid, **2008**.
- 398 (12) Quindós L.S; Fernandez P.L; Soto J; Ródenas C; Terrestrial gamma radiation levels
399 outdoors in Cantabria, Spain. *Journal of Radiological Protection* **1991**, 11, 127-130
- 400 (13) González-Díez A; Soto J; Gómez J; Bonachea J; Martínez-Díaz J; Cuesta J.A; Olague I;
401 Remondo J; Fernández Maroto F; Díaz de Terán J.R Identification of latent faults using
402 a radon test. *Geomorphology* **2009**, 110, 11-19
- 403 (14) Gutiérrez, J. L.; Sainz, C.; Fuente I.; Quindós, L.; Quindós J.; Fernández, A.; Casal S.;
404 Lopez, D.; Arteché, D.; Fernández, E.; Quindós, L. S. International intercomparison
405 exercise on natural radiation measurements under field conditions. **2012**, PubliCan Ed.
406 Universidad de Cantabria. ISBN: 978-84-86116-64-4

- 407 (15) Cosma C.; Moldovan M.; Dicu T.; Kovacs T.; Radon in water from Transilvania.
408 Radiation Measurements **2008**, 43, 1423-1428
- 409 (16) Kowalczyk, A. J.; Froelich, P. N. Cave air ventilation and CO₂ outgassing by radon-222
410 modeling: How fast do caves breathe?. *Earth and Planetary Science Letters*. **2010**, 289,
411 209–219; DOI 10.1016/j.epsl.2009.11.010.
- 412 (17) International Commission on Radiological Protection. **1993**. Protection against radon-
413 222 at home and at work. Oxford: Pergamon Press; ICRP Publication 65; Annals of ICRP
414 23 (2).
- 415 (18) UNSCEAR. *Effects of ionizing radiation, UNSCEAR 2006 Report*; United Nations
416 Scientific Committee on the Effects of Atomic Radiation: New York, **2008**; *Volume II:*
417 *Annex E*.
- 418 (19) Hunyadi, I.; Csige, J.; Hakl, E.; Baradacs, J.; Dezso, Z. Temperature dependence of the
419 calibration factor of radon and radium determination in water samples by SSNTD.
420 *Radiation Measurements*. **1999**, 31 (1), 301-306; DOI 10.1016/S1350-4487(99)00139-
421 0.
- 422 (20) Quindós L. S.; Sainz, C.; Fuente, I.; Gutierrez, J. L.; Fernandez, A.; Quindós, L.
423 Fernandez, E. A prototype for a more accurate evaluation of radon exposure in
424 workplaces, 12th International Workshop on the Geological Aspects of Radon Risk
425 Mapping, Prague, Czech Republic, Sept 16–19, **2014**.
- 426 (21) Soto, J.; Delgado, M. T.; Fernandez, P.; Gómez, J.; Quindós L. S.; Niveles de ²²²Rn en
427 el balneario Las Caldas de Besaya (Cantabria). *Rec. San. Sig. Pub.* **1991**, 65, 71-75.
- 428 (22) Soto, J.; Fernandez, P.; Quindós, L. S.; Gómez J. Radioactivity in Spanish spas. *The*
429 *Science of the Total Environment*. **1995**, 162, 187-192.

430 (23) Spain. Reglamento sobre protección sanitaria contra radiaciones ionizantes. Título IV.
431 Principios fundamentales de protección operacional de los trabajadores expuestos,
432 personas en formación y estudiantes para la ejecución de las prácticas. *BOE*, July 26,
433 **2001**, num. 178, 27288-27292.

434 .

435

436 TABLES

437 **Table 1.** Results of the parameters which characterize the equations given by CCM and OCM
 438 models obtained through fitting the experimental data on the dates indicated.

Date	CCM				OCM			
	C_0^a (Bq/l)	ϕ (Bq/l h ⁻¹)	λ (h ⁻¹)	R ^{2b}	C_1^a (Bq/l)	d (Bq/l h ⁻¹)	λ^* (h ⁻¹)	R ^{2b}
March 14-15	581	222 ± 11	0.31 ± 0.02	0.99	710	450 ± 20	0.76 ± 0.03	0.98
April 25-26	601	170 ± 10	0.24 ± 0.02	0.97	660	310 ± 20	0.52 ± 0.03	0.99
May 13-14	557	270 ± 30	0.40 ± 0.04	0.94	657	420 ± 30	0.72 ± 0.05	0.99
June 19-20	585	280 ± 30	0.40 ± 0.04	0.96	650	470 ± 30	0.80 ± 0.05	0.99
July 7-8	534	230 ± 20	0.33 ± 0.03	0.96	619	370 ± 50	0.70 ± 0.09	0.99
August 2-3	533	320 ± 30	0.48 ± 0.04	0.97	703	420 ± 20	0.67 ± 0.04	0.96

439 ^aInitial concentration taken as fixed parameter, which uncertainty is 3%. ^bAdjusted coefficient of determination
 440 R²-adj

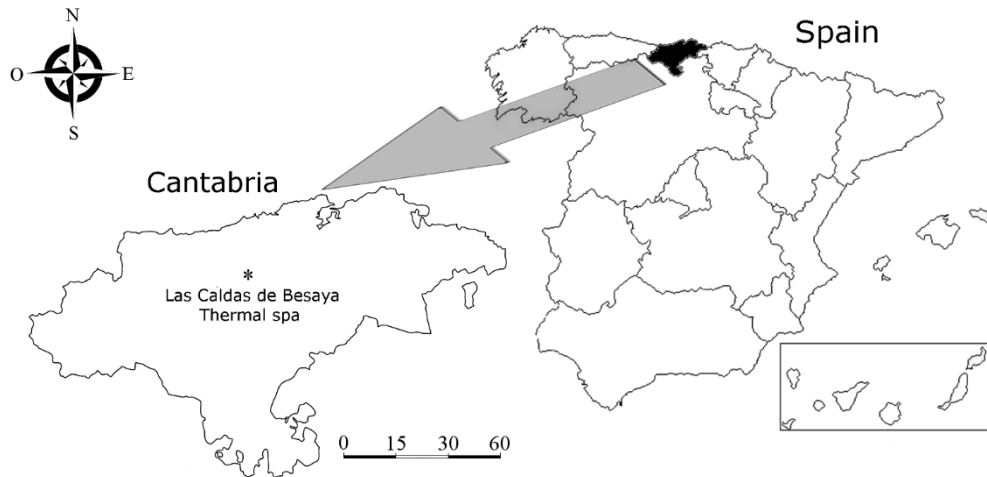
441

442 **Table 2.** Parameter results of λ_v , λ_l and C^* obtained from equations 3 and 6 and data shown
 443 in Table 2. Uncertainty in values was achieved through propagation of errors.

Series	λ_v (h ⁻¹)	λ_l (h ⁻¹)	C^* (Bq/l)
March	0.43 ± 0.01	0.32 ± 0.03	430 ± 80
April	0.23 ± 0.02	0.28 ± 0.04	500 ± 100
May	0.39 ± 0.04	0.32 ± 0.06	470 ± 160
June	0.39 ± 0.04	0.40 ± 0.06	480 ± 130
July	0.32 ± 0.03	0.37 ± 0.09	380 ± 170
August	0.47 ± 0.04	0.19 ± 0.06	500 ± 200

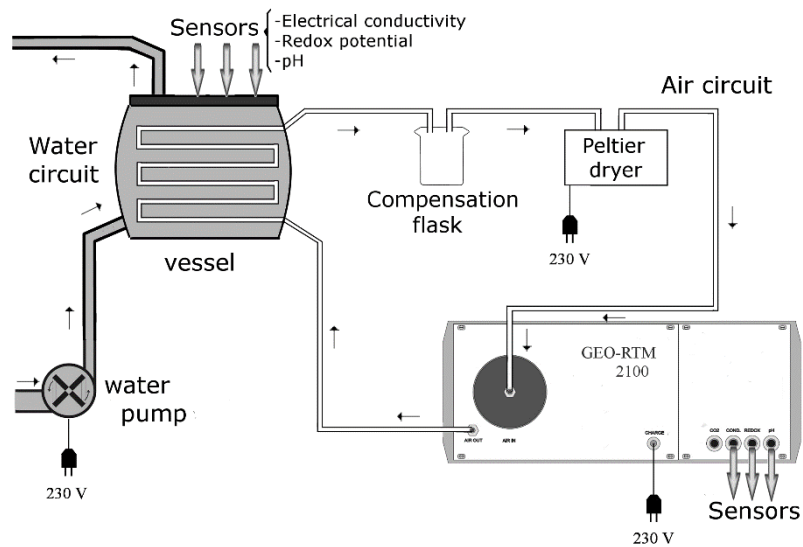
444

445



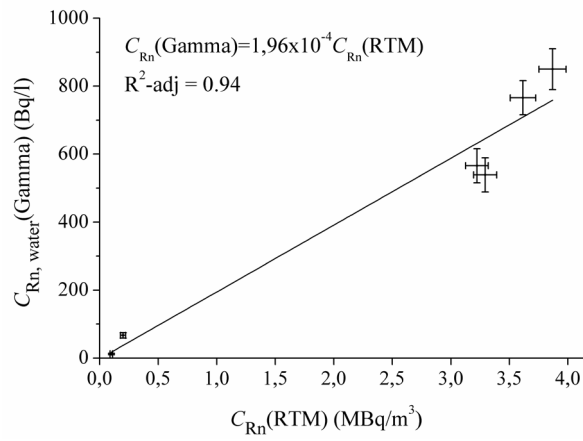
450 **Figure 1.** Location of Las Caldas de Besaya thermal spa, Cantabria, Spain.

150 x 66 mm (300 x 300 dpi)



454 **Figure 2.** Experimental device diagram used for continuous measurement of radon in water.

110x80 mm (600x600 dpi)



457

458 **Figure 3.** Radon concentration obtained with gamma spectrometry $C_{Rn, \text{water}}(\text{gamma})$ versus
 459 obtained with RTM 2100 device $C_{Rn}(\text{RTM})$.

460

82.5x58 (1200x1200 dpi)

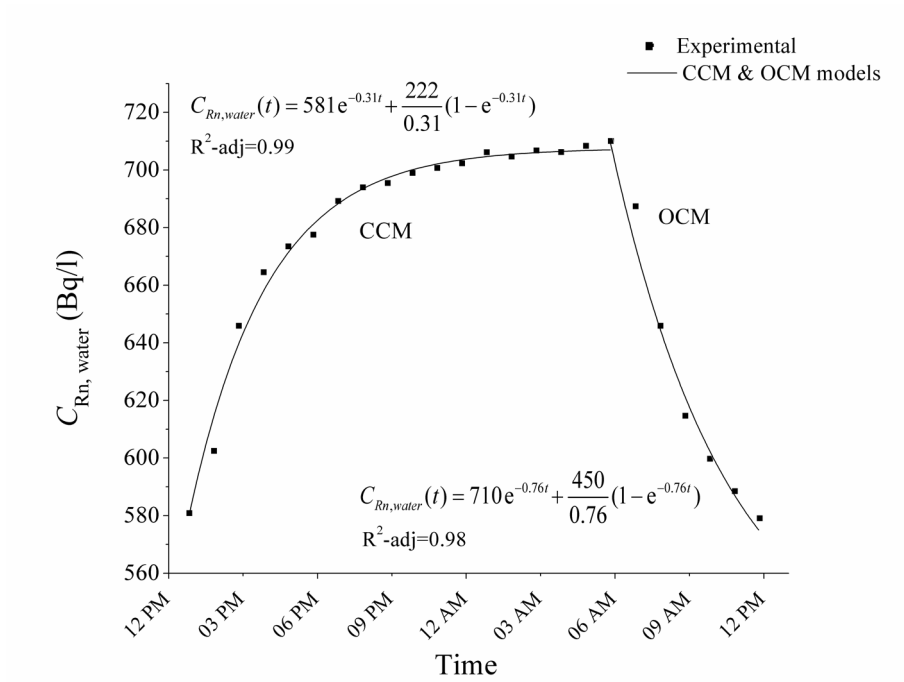
461

462

463

464

465



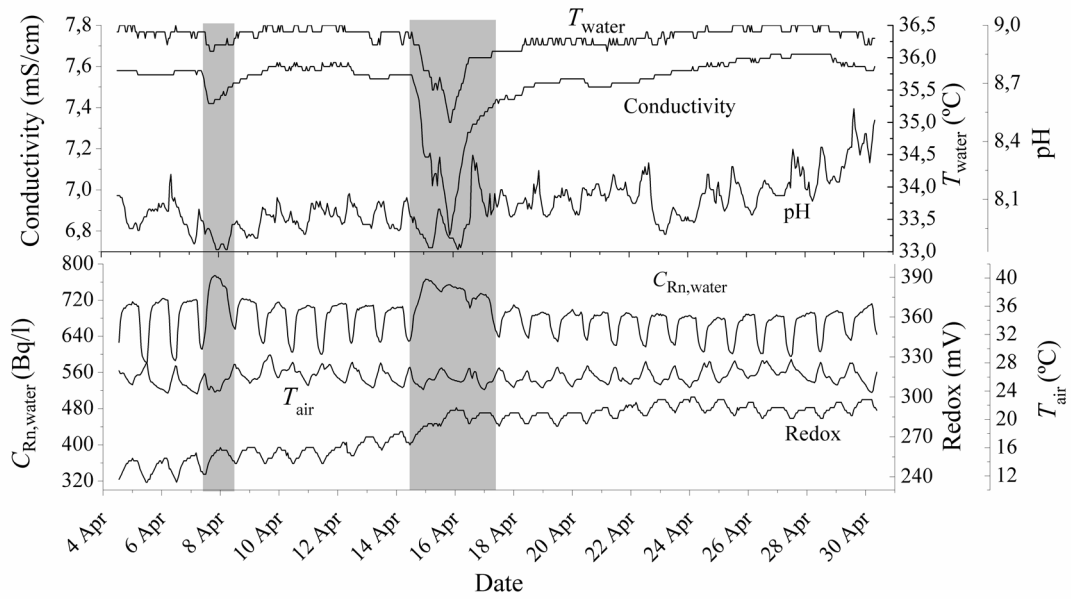
466

467 **Figure 4.** Fit made according to the CCM and OCM models to experimental data on the radon
468 concentration in water from 14th (12:50 PM.) to 15th (11:50 AM.) March.

469

120x90 mm (1200x1200 dpi)

470



471

472 **Figure 5.** Experimental results of radon concentration in water, conductivity, redox potential,
 473 pH and water and air temperatures measured in April with RTM 2100 device.

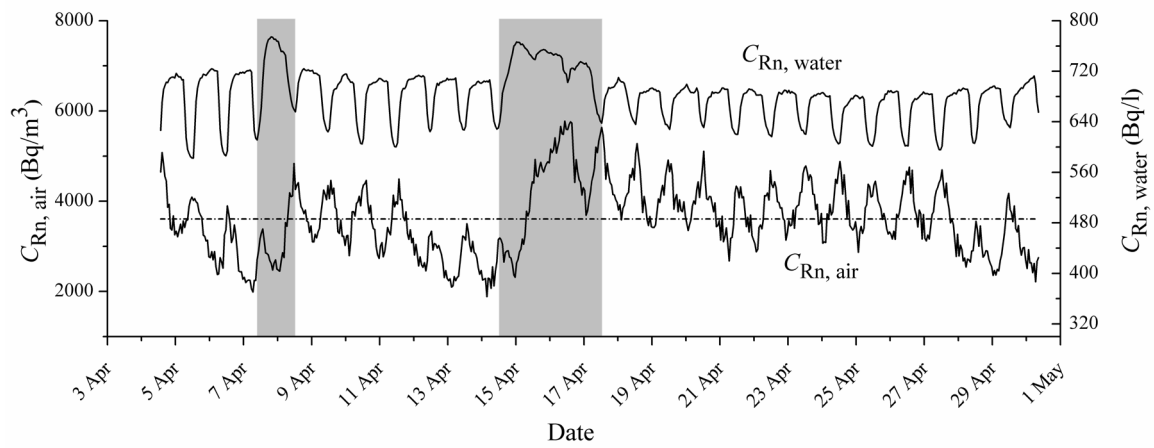
474

155x85 mm (1200x1200 dpi)

475

476

477



478

479 **Figure 6.** Radon concentration in water and air time series for April, 2012 measured with RTM
 480 2100 and Radon Scout devices respectively. Dashed line indicates monthly average for radon
 481 in air which value is 3600 Bq/m³.

482

155x72 mm (1200x1200 dpi)

483

484

485

